

# Effects of TiO<sub>2</sub> Addition on Kinetics of *In Situ* Spinel Formation and Properties of Alumina-Magnesia Refractory Castables

W. Yuan\*, H. Tang, H. Shang, J. Li, C. Deng, H. Zhu

The State Key Laboratory of Refractories and Metallurgy, Wuhan University  
of Science and Technology, Wuhan 430081, China

received November 2, 2016; received in revised form December 18, 2016; accepted January 25, 2017

## Abstract

This work addresses the effects of TiO<sub>2</sub> addition on the kinetics of *in situ* spinel formation and the properties of alumina-magnesia refractory castables. The kinetics of the formation of spinel in alumina-magnesia refractory castables with TiO<sub>2</sub> addition (0–3 wt%) during firing at 1250–1450 °C for different times was investigated by means of XRD analysis. The reaction rate constant and apparent activation energy of spinel formation in castables calculated based on the Ginstling-Braunstein model varied with the firing temperature and TiO<sub>2</sub> addition. A comparison of the castables' properties including permanent linear changes, apparent porosity and strength was discussed. The results demonstrated that the *in situ* reactions and properties of the alumina-magnesia refractory castables depend on the combined effects of TiO<sub>2</sub>.

*Keywords:* Castables, kinetic, spinel, reaction, properties

## I. Introduction

Refractories are trans-scale multi-component and heterogeneous materials. One important development trend in refractories is the increase in unshaped monolithic refractories. Due to their excellent properties, such as high mechanical strength and corrosion resistance, alumina-magnesia refractory castables have been widely used in the wall and bottom impact pad of steel ladles<sup>1</sup>. The performance of alumina-magnesia refractory castables was optimized with the introduction of novel aggregates<sup>2–4</sup>. However, tailoring the microstructure and properties of castables with additives proved a low-cost alternative<sup>5</sup>. The formation of spinel as a consequence of the reaction between magnesia and alumina at high temperatures was associated with a volume expansion of 8 %<sup>6</sup>. The use of mineralization could increase strength, thermal shock resistance and other properties of refractories<sup>7</sup>. TiO<sub>2</sub> is one of the most effective multifunctional mineralizers as it can speed up spinel formation and promote the densification of castables<sup>8</sup>. In order to accurately control the properties of castables, the effects of TiO<sub>2</sub> on the *in situ* reactions in castables should be taken into account and quantitatively evaluated. Because of the limitation of thermodynamic equilibria based on phase diagrams for refractories<sup>9</sup>, the dynamic aspect had to be considered. However, the correlation between the mineralizer TiO<sub>2</sub> and phase evolution as well as properties of castables was very complex. Previous works focused on the changes in phase composition and properties of alumina-magnesia refractory castables with TiO<sub>2</sub> in the range from 0.5 to 2 wt% after calcining at elevated temperatures for 5 h<sup>8,10</sup>. Spinel for-

mation was controlled by an inter-diffusion mechanism of ions<sup>11</sup>, which also strongly depended on the reaction time. It was revealed that the densification rate of the magnesia-alumina system was increased with TiO<sub>2</sub> addition, which demonstrated that the kinetics of reaction sintering of compacted oxide mixture samples had been changed<sup>12</sup>. But the kinetics of spinel formation in alumina-magnesia cement-bonded castables comprising multi-components (magnesia, tabular and calcined alumina) with a wide size distribution lacked research. In this study, the effects of TiO<sub>2</sub> addition (up to 3 wt%) on the kinetics of *in situ* spinel formation and the properties of alumina-magnesia refractory castables fired at 1250–1450 °C for different times were investigated.

## II. Materials and Methods

Alumina-magnesia castables were prepared according to the compositions listed in Table 1. The added water content for vibrocasting was in the range of 4.5–4.7 wt%. All vibrocastables were cast, and then cured at 25 °C for 24 h with relative humidity of 100 %, followed by drying at 110 °C for 24 h. Samples were calcined at 1250–1450 °C for 30–300 min, respectively. The permanent linear change (PLC) was measured in compliance with GB/T 5988–2007. The apparent porosity of the castables was measured with the Archimedes technique. The cold modulus of rupture (CMOR) for castables was measured in a three-point bending test in accordance with GB/T 3001–2007. The phase composition of castables was analyzed by means of X-ray diffraction (XRD, Philips, X'pert Pro MPD, Netherlands). The degree of conversion of spinel was calculated based on the RIR method<sup>13</sup>. The microstructure of the fired castables was

\* Corresponding author: [yuanwenjie@wust.edu.cn](mailto:yuanwenjie@wust.edu.cn)

characterized with scanning electron microscopy (SEM, JEOL JSM-6610, Japan) and an energy-dispersive spectrometer (EDS, Bruker QUANTAX200–30, Germany).

**Table 1:** Composition of alumina-magnesia refractory castables.

Raw materials	Content (wt%)				
	T0	T0.5	T1	T2	T3
Tabular alumina ( $\leq 6$ mm) (Almatis)	61	61	61	60	60
Tabular alumina ( $\leq 200$ mesh) (Almatis)	19	18.5	18	18	17
Reactive alumina (CL370) (Almatis)	7	7	7	7	7
Calcined magnesia (180 mesh)	6	6	6	6	6
Calcium aluminate cement (Secar71) (Kerneos)	6	6	6	6	6
Silicon fume (951U) (Elkem)	1	1	1	1	1
TiO <sub>2</sub>	0	0.5	1	2	3

**III. Results and Discussion**

As the formation of spinel from its constituent oxides was diffusion-controlled<sup>7</sup>, the function between the reaction

rate constant and time can be described with the Ginstling-Braunstein model<sup>14</sup>:

$$g(\alpha) = 1 - 2\alpha/3 - (1-\alpha)^{2/3} = kt$$

where  $a$  is the degree of conversion, and  $k$  is the reaction rate constant. The effects of the firing temperature and time on  $g(a)$  of spinel in castables are shown in Fig. 1. It can be seen that the slope of the fitting curves based on the Ginstling-Braunstein model stands for the reaction rate constant increase with the addition of TiO<sub>2</sub> at 1250 °C. The reaction rate constant of the castables containing TiO<sub>2</sub> presented a significant difference to that of the reference composition fired at 1350 °C and 1450 °C. The maximum reaction rate constant was achieved in sample T2 after firing at 1450 °C.

The activation energy  $E$  of the reaction was calculated from the Arrhenius expression:

$$k = A \cdot \exp(-E/RT)$$

where  $A$  is the frequency factor and  $R$  is the gas constant. The logarithm of the reaction rate constant  $\ln k$  for spinel is plotted against  $1000/T$  in Fig. 2. The apparent activation energy of spinel formation in alumina-magnesia refractory castables derived from the Arrhenius equation was between 100.8 and 328.3 kJ/mol at the temperature range from 1250 to 1450 °C as listed in Table 2. It is worth noting that the relationship between the apparent activation energy of spinel formation and the amount of TiO<sub>2</sub> was not simply linear, which will be discussed in a later section.

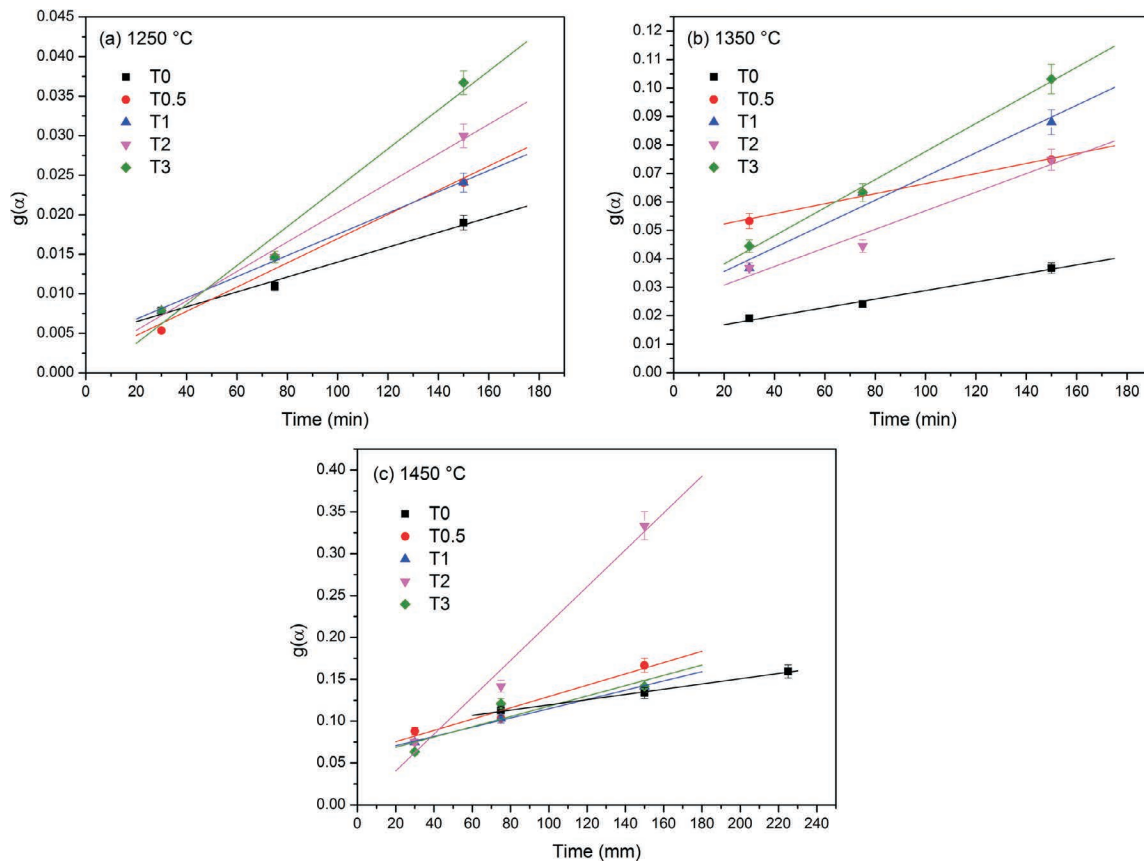


**Fig. 1:**  $g(\alpha)$  of spinel in alumina-magnesia refractory castables after calcining at 1250 °C (a), 1350 °C (b) and 1450 °C (c).

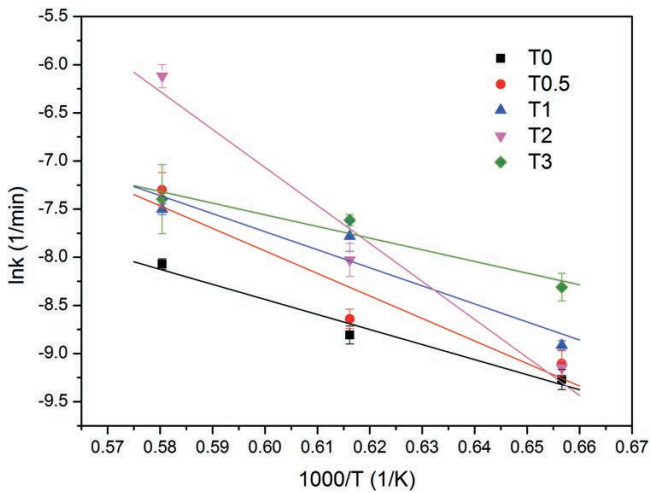


**Fig. 2:** Plots  $\ln k$  vs.  $1000/T$  for spinel in alumina-magnesia refractory castables.

There was no diffraction peak for the castable containing a Ti element such as  $\text{TiO}_2$  and  $\text{CaTiO}_3$  in the XRD patterns of the alumina-magnesia refractory castables after calcining at  $1450^\circ\text{C}$  for different times from 30 to 300 min as shown in Fig. 3, which indicates that  $\text{TiO}_2$  as a mineralizer fully reacted with other components in the casta-

bles at high temperatures. The major phases in the fired castables were composed of corundum, spinel and  $\text{CA}_6$ . The changes of the diffraction peak's position for spinel (311) and  $\text{CA}_6$  (114) compared with the corundum (104) peak in castables fired at  $1450^\circ\text{C}$  are shown in Fig. 4. It was demonstrated that the solid-soluted content of these two phases depended on the  $\text{TiO}_2$  addition. The spinel peaks shifted to a higher angle with increasing holding time, which represented more  $\text{Al}_2\text{O}_3$  dissolved into the spinel. As the offset of the spinel peak for samples T0.5 and T1 was less than the reference sample T0, it was deduced that the dissolution of  $\text{TiO}_2$  into spinel solid solution was more prominent in castables with 0.5 and 1 wt%  $\text{TiO}_2$ . On the contrary, the peaks of  $\text{CA}_6$  gradually shifted to a lower angle with  $\text{TiO}_2$  addition, which was attributed to the solid solution of Ti and Mg atoms. It was evidenced that the dependence of the distribution of Ti element in spinel and  $\text{CA}_6$  on the firing time as well as the temperature was governed by the  $\text{TiO}_2$  addition. Moreover, the other major function of  $\text{TiO}_2$  was the modification of sintering<sup>15</sup>. Therefore, the apparent activation energy of the spinel formation in alumina-magnesia refractory castables presented a non-monotonous change with the addition of  $\text{TiO}_2$ .

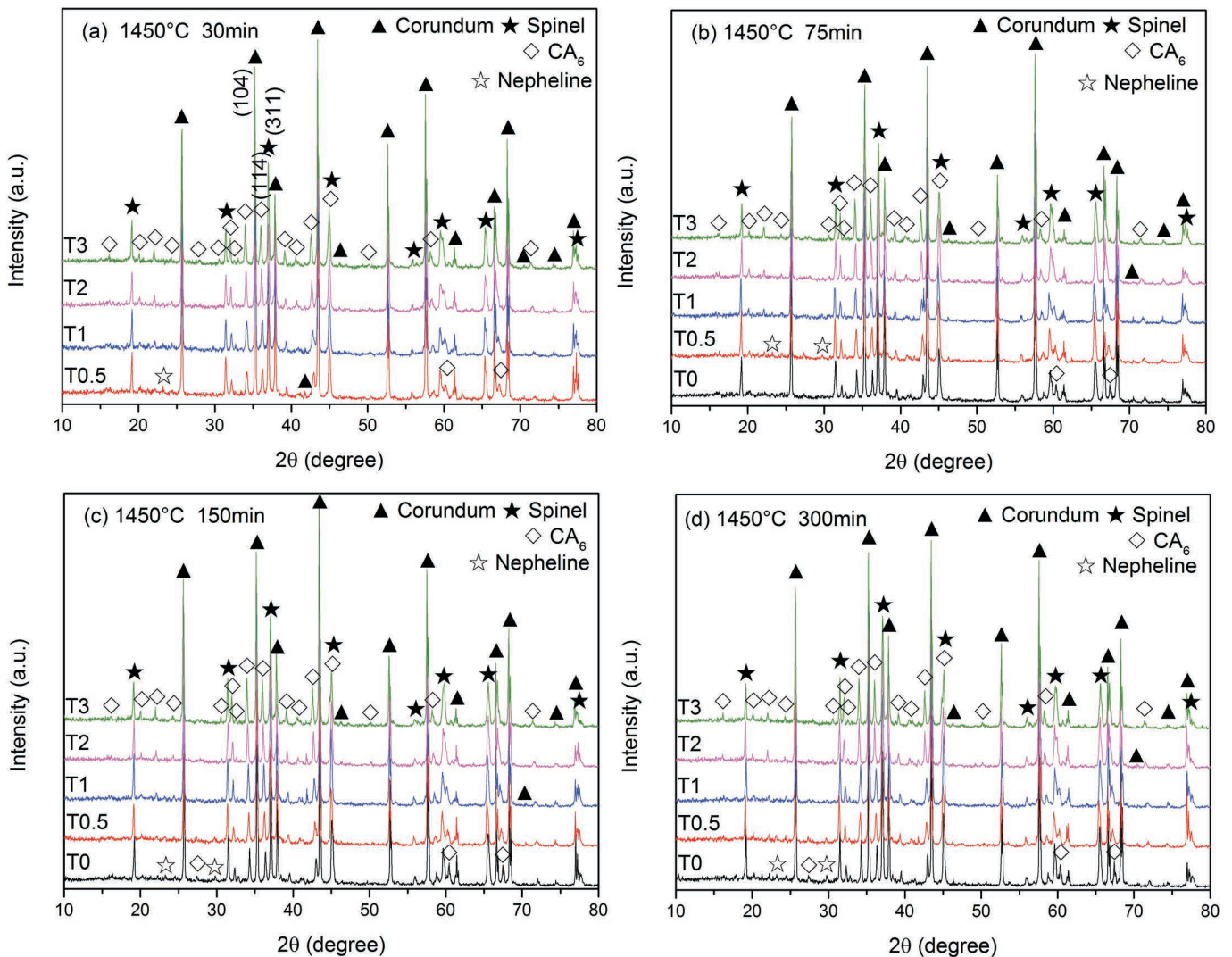


**Fig. 3:** XRD patterns of alumina-magnesia refractory castables after calcining at  $1450^\circ\text{C}$ : (a) 30 min, (b) 75 min, (c) 150 min and (d) 300 min.

**Table 2:** Apparent activation energy  $E_a$  of spinel in alumina-magnesia refractory castables with  $TiO_2$  addition.

No.	$E_a$ (kJ/mol)
T0	$129.9 \pm 11.0$
T0.5	$194.5 \pm 31.0$
T1	$155.8 \pm 24.1$
T2	$328.3 \pm 30.6$
T3	$100.8 \pm 13.3$

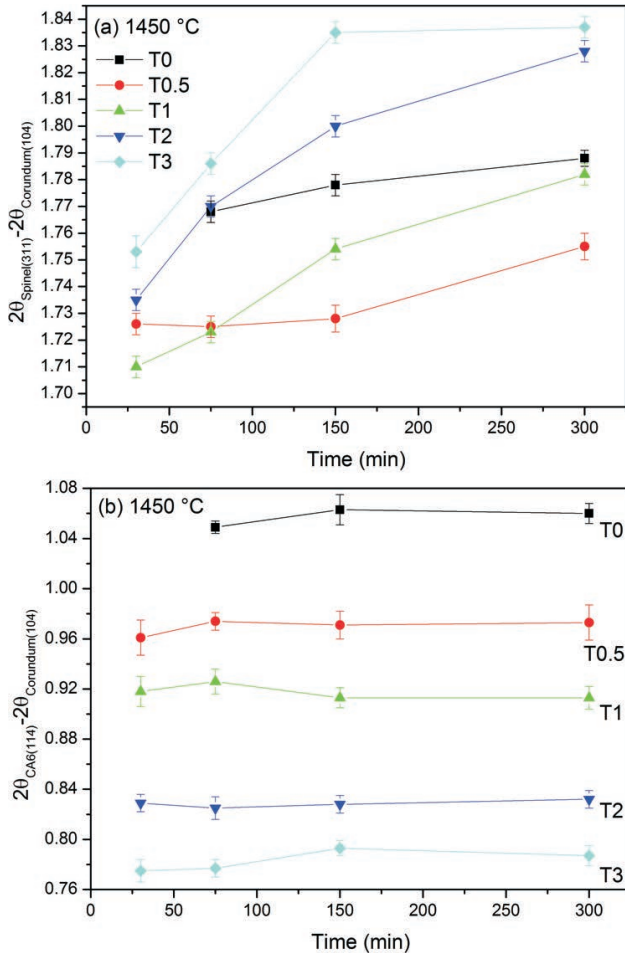


**Fig. 4:** The position shift of the diffraction peaks for spinel in alumina-magnesia refractory castables after calcining at 1450 °C: (a) spinel and (b)  $Ca_6$

Controlling the expansion behavior of alumina-magnesia castables was essential to maintain the integrity of the component during use. Fig. 5 presents permanent linear changes of castables after calcining at 1250–1450 °C. The expansion of castables with 0.5 wt% of  $TiO_2$  addition was slightly greater than that of the referenced castable T0. In general, the expansion of sample T1 achieved the highest value at 1250 and 1350 °C except for 300 min. In contrast, the expansion of sample T2 was basically less than that of sample T1. Especially castables containing 2 wt% (holding time  $\geq 75$  min) and 3 wt%  $TiO_2$  presented a certain amount of shrinkage after firing at 1450 °C. The shrinkage of sintering could completely counterbalance the expansion derived from *in situ* reactions when more  $TiO_2$  was added.

Thus, the expansion behavior of alumina-magnesia castables depended not only on the phase formation but also the sintering.

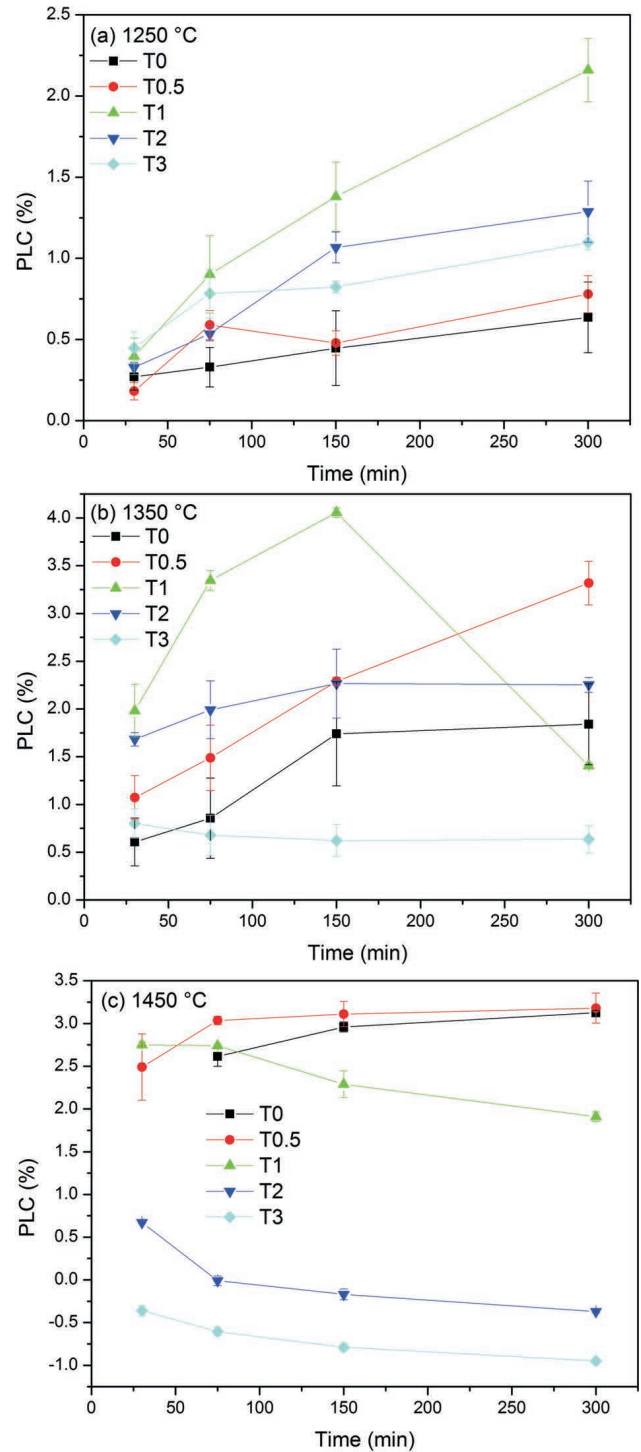


**Fig. 5:** Permanent linear changes of alumina-magnesia refractory castables after calcining at 1250 °C (a), 1350 °C (b) and 1450 °C (c).

The variation of the apparent porosity for castables containing  $TiO_2$  with the calcining temperature and time presented a similar trend as the PLC as shown in Fig. 6. The greater expansion of the castables resulted in higher porosity. The apparent porosity of castables with 2 wt% and 3 wt% after firing at 1450 °C was reduced dramatically, which was possibly related to the phase evolution in castables.

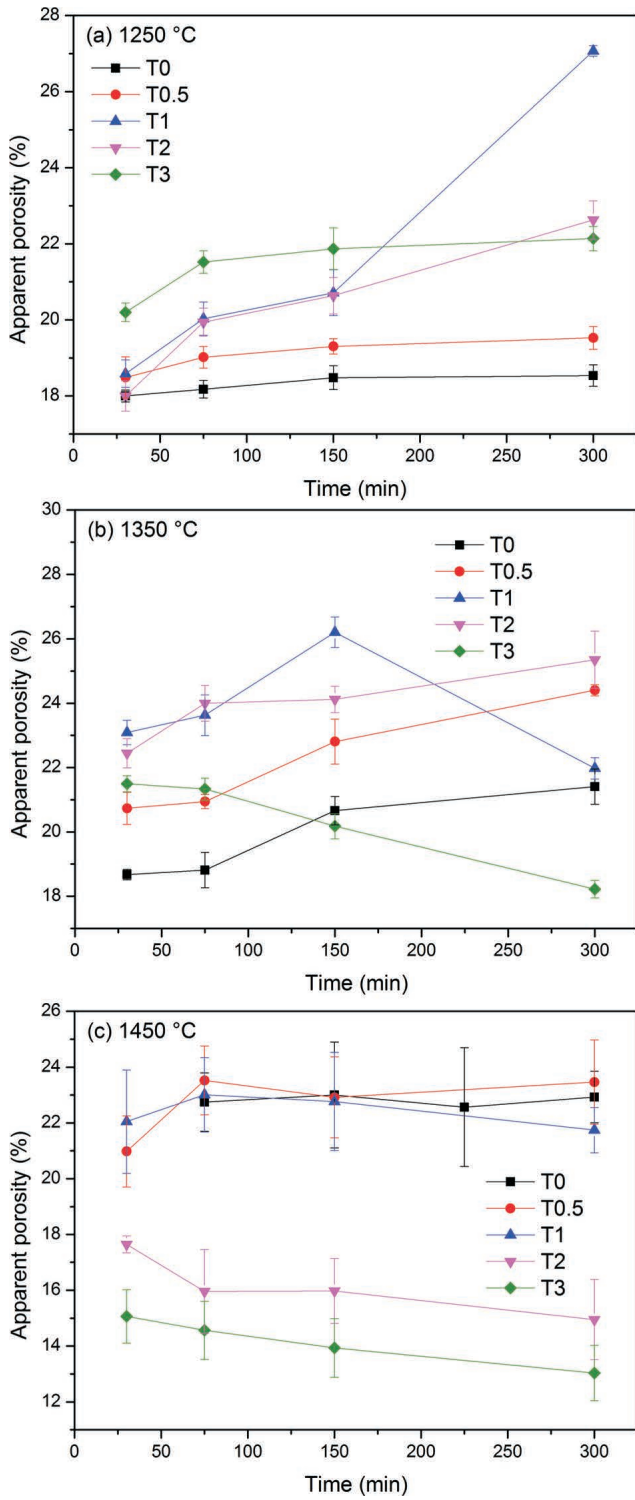


Fig. 6: Apparent porosity of alumina-magnesia refractory castables after calcining at 1250 °C (a), 1350 °C (b) and 1450 °C (c).

In Fig. 7, the significant difference in strength for castables containing TiO<sub>2</sub> at room temperature is presented. The cold modulus of rupture for castables with TiO<sub>2</sub> addition after firing at 1250 °C was less than that for the referenced castables as a result of their high apparent porosity. Because the bonding between different phases was enhanced by the formation of spinel and CA<sub>6</sub> solid solution in castables containing TiO<sub>2</sub>, the contribution of the bonding to the strength of the castables became more dominant at higher temperatures.

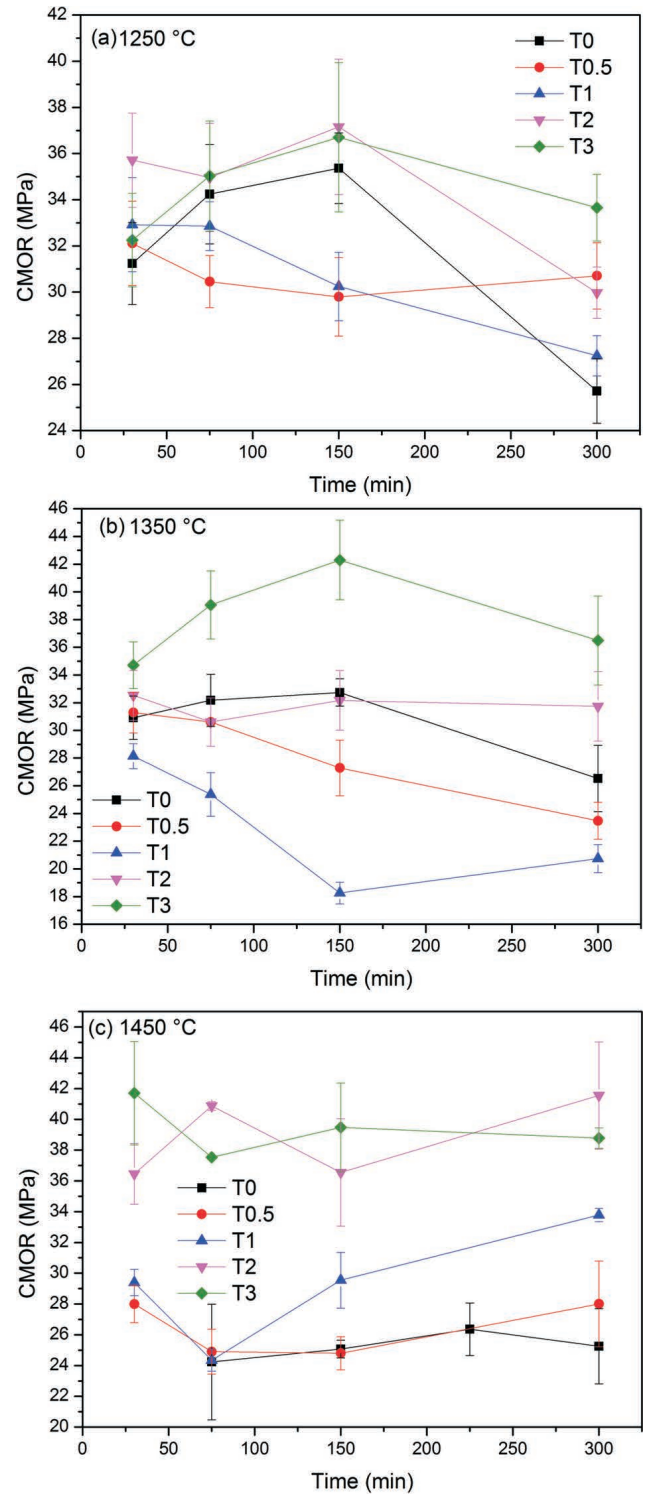


Fig. 7: Cold modulus of rupture (CMOR) of alumina-magnesia refractory castables after calcining at 1250 °C (a), 1350 °C (b) and 1450 °C (c).

Figs. 8(a)-(e) show SEM images of alumina-magnesia refractory castables after calcining at 1450 °C for 5 h. It can be observed that there were coarse CA<sub>6</sub> platelets in the castables without TiO<sub>2</sub> (Fig. 8(a)). The addition of 0.5–2 wt% TiO<sub>2</sub> resulted in much finer CA<sub>6</sub> grains (Fig. 8(b)-(d)). The spinel and CA<sub>6</sub> in the matrix of the castables were bonded tightly in the case of TiO<sub>2</sub> addition up to 3 wt%. Both spinel and CA<sub>6</sub> are not even recognizable from Fig. 8(e).

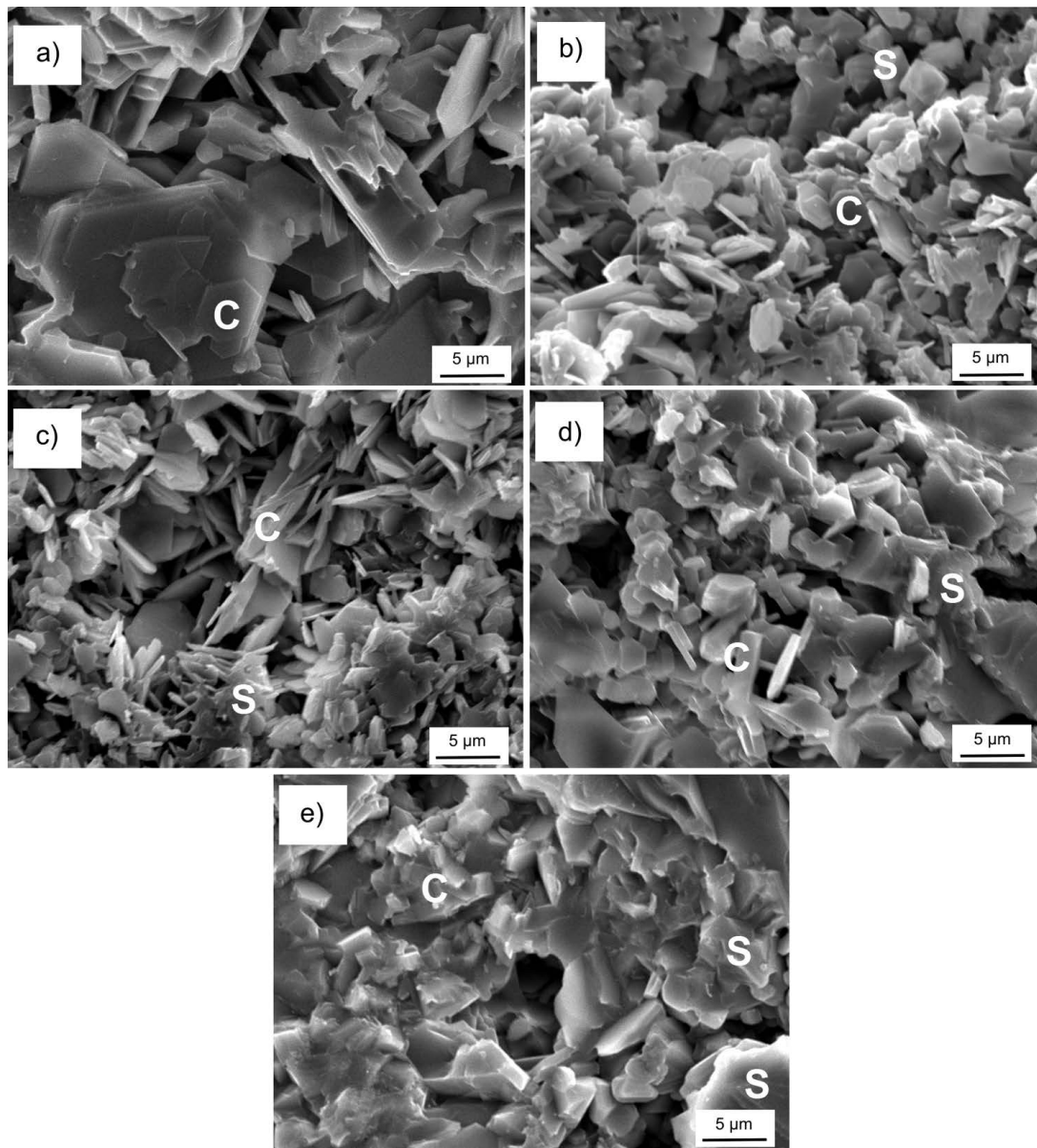


Fig. 8: SEM images of alumina-magnesia refractory castables after calcining at 1450 °C for 5 h: (a) T0, (b) T0.5, (c) T1, (d) T2 and (e) T3 (C-CA<sub>6</sub> and S-spinel).

#### IV. Conclusions

The effects of the addition of TiO<sub>2</sub> on the kinetics of *in situ* spinel formation and the properties of alumina-magnesia refractory castables were investigated. The reaction rate constant of the spinel formation depended on the addition of TiO<sub>2</sub> as well as the firing temperature. The apparent activation energy of the spinel formation presented a non-monotonous change with TiO<sub>2</sub> addition as a consequence of the variation of Ti distribution in the spinel and CA<sub>6</sub>. A small amount of added TiO<sub>2</sub> (0.5–2 %) resulted in higher expansion and apparent porosity of castables after firing at 1250 and 1350 °C. Castables with higher TiO<sub>2</sub> content (2–3 %) fired at 1450 °C presented a certain amount of shrinkage, and possessed lower porosity as well as higher strength. Moreover, the comprehensive effects of TiO<sub>2</sub> as a mineralizer need to be considered for the design of engineered castables.

#### Acknowledgment

This research was financially supported by the National Nature Science Foundation of China (No. 51502214 and 51574187).

#### References

- 1 Braulio, M.A.L., Rigaud, M., Buhr, A., Parr, C., Pandolfelli, V.C.: Spinel-containing alumina-based refractory castables, *Ceram. Int.*, **37**, 1705–1724, (2011).
- 2 Liang, Y.H., Huang, A., Zhu, X.W., Gu, H.Z., Fu, L.P.: Dynamic slag/refractory interaction of lightweight Al<sub>2</sub>O<sub>3</sub>-MgO castable for refining ladle, *Ceram. Int.*, **41**, [6], 8149–8154, (2015).
- 3 Fu, L.P., Gu, H.Z., Huang, A., Zhang, M.J., Hong, X.Q., Jin L.W.: Possible improvements of alumina-magnesia castable by lightweight microporous aggregates, *Ceram. Int.*, **41**, [1], 1263–1270, (2015).
- 4 Fu, L.P., Gu, H.Z., Huang, A., Zhang, M.J., Li, Z.K.: Slag resistance mechanism of lightweight microporous corundum aggregate, *J. Am. Ceram. Soc.*, **98**, [5], 1658–1663, (2015).

- 5 Braulio, M.A.L., Pandolfelli, V.C.: Tailoring the microstructure of cement-bonded alumina-magnesia refractory castables, *J. Am. Ceram. Soc.*, **93**, [10], 2981–2985, (2010).
- 6 Rigaud, M., Palco, S., Wang, N.: Spinel formation in the MgO-Al<sub>2</sub>O<sub>3</sub> system relevant to basic oxides, in: *Proceedings of UNITECR'95*, Kyoto, Japan, 387–394, (1995).
- 7 Semler, C.E.: Refractories – the world's most important but least known products, *Am. Ceram. Soc. Bull.*, **93**, [2], 34–39, (2014).
- 8 Yuan, W.J., Deng, C.J., Zhu, H.X.: Effects of TiO<sub>2</sub> addition on the expansion behavior of alumina-magnesia refractory castables, *Mater. Chem. Phys.*, **162**, 724–733, (2015).
- 9 Lee, W.E., Argent, B.B., Zhang, S.: Complex phase equilibria in refractories design and use, *J. Am. Ceram. Soc.*, **85**, [12], 2911–2918, (2002).
- 10 Yuan, W.J., Deng, C.J., Zhu, H.X.: The influence of TiO<sub>2</sub> addition on the modulus of rupture of alumina-magnesia refractory castables, *J. Mater. Eng. Perform.*, **24**, 3100–3106, (2015).
- 11 Sako, E.Y., Braulio, M.A.L., Zinngrebe, E., Laan, S.R. van der, Pandolfelli, V.C.: Fundamentals and applications on *in situ* spinel formation mechanisms in Al<sub>2</sub>O<sub>3</sub>-MgO refractory castables, *Ceram. Int.*, **38**, 2243–2251, (2012).
- 12 Sinhamahapatra, S., Kausik Dana, K., Ghosh, A., Reddy, V.P., Tripathin, H.S.: Dynamic thermal study to rationalize the role of titania in reaction sintering of magnesia-alumina system, *Ceram. Int.*, **41**, 1073–1078, (2015).
- 13 Snyder, R.L.: The use of reference intensity ratios in X-ray quantitative analysis, *Powder Diffr.*, **7**, [4], 186–193, (1992).
- 14 Lu, C.H., Wu, P.C.: Reaction mechanism and kinetic analysis of the formation of Sr<sub>2</sub>SiO<sub>4</sub> via solid-state reaction, *J. Alloy. Compd.*, **466**, 457–462, (2008).
- 15 Maitra, S., Das, S., Sen, A.: The role of TiO<sub>2</sub> in the densification of low cement Al<sub>2</sub>O<sub>3</sub>-MgO spinel castable, *Ceram. Int.*, **33**, 239–243, (2007).

